Phosphorylation of Crm1 by CDK1–cyclin-B promotes Ran-dependent mitotic spindle assembly

Zhige Wu[1,2], Qing Jiang[1], Paul R. Clarke[2,*] and Chuanmao Zhang[1,*]

[1]The MOE Key Laboratory of Cell Proliferation and Differentiation and the State Key Laboratory of Bio-membrane and Membrane Bio-engineering, College of Life Sciences, Peking University, Beijing 100871, China
[2]Division of Cancer Research, Medical Research Institute, Jacqui Wood Cancer Centre, Ninewells Hospital and Medical School, University of Dundee, Dundee DD1 9SY, UK

*Authors for correspondence (p.r.clarke@dundee.ac.uk; zhangcm@pku.edu.cn)

Accepted 13 May 2013
Journal of Cell Science 126, 3417–3428
© 2013. Published by The Company of Biologists Ltd
doi: 10.1242/jcs.126854

Summary

Mitotic spindle assembly in animal cells is orchestrated by a chromosome-dependent pathway that directs microtubule stabilization. RanGTP generated at chromosomes releases spindle assembly factors from inhibitory complexes with importins, the nuclear transport factors that facilitate protein import into the nucleus during interphase. In addition, the nuclear export factor Crm1 has been proposed to act as a mitotic effector of RanGTP through the localized assembly of protein complexes on the mitotic spindle, notably at centrosomes and kinetochores. It has been unclear, however, how the functions of nuclear transport factors are controlled during mitosis. Here, we report that human Crm1 is phosphorylated at serine 391 in mitosis by CDK1–cyclin-B (i.e. the CDK1 and cyclin B complex). Expression of Crm1 with serine 391 mutated to either non-phosphorylated or phosphorylation-mimicking residues indicates that phosphorylation directs the localization of Crm1 to the mitotic spindle and facilitates spindle assembly, microtubule stabilization and chromosome alignment. We find that phosphorylation of Crm1 at serine 391 enhances its RanGTP-dependent interaction with RanGAP1–RanBP2 and promotes their recruitment to the mitotic spindle. These results show that phosphorylation of Crm1 controls its molecular interactions, localization and function during mitosis, uncovering a new mechanism for the control of mitotic spindle assembly by CDK1–cyclin-B. We propose that nuclear transport factors are controlled during mitosis through the selection of specific molecular interactions by protein phosphorylation.

Key words: Crm1, Ran, Mitosis, Mitotic spindle, Phosphorylation

Introduction

Ran, a nuclear small GTPase of Ras superfamily, regulates a number of diverse functions associated with the nucleus and chromosomes, including nuclear transport, DNA replication, nuclear envelope formation and mitotic spindle assembly (Clarke and Zhang, 2008). The GTP–GDP cycle of Ran is regulated by the nucleosome-binding protein RCC1, which acts as a nucleotide exchange factor for Ran (RanGEF) (Bischoff and Ponstingl, 1991), and a cytoplasmic GTPase-activating protein, RanGAP1 (Bischoff et al., 1994). During interphase, RCC1 catalyzes the exchange of GDP to GTP on Ran to generate RanGTP in the nucleus, while RanGAP1, together with RanBP1 or RanBP2, stimulates the hydrolysis of GTP on Ran to generate RanGDP in the cytoplasm (Görlich et al., 1996).

The relatively high concentration of RanGTP in the nucleus causes the assembly of nuclear export complexes formed between proteins carrying a leucine-rich nuclear export signal (NES) with nuclear export factors, notably Crm1, also known as exportin 1 or Xpo1 (Fornerod et al., 1997a; Fukuda et al., 1997; Ossareh-Nazari et al., 1997; Stade et al., 1997). Following transit through the nuclear pores, the trimeric complex between RanGTP, Crm1 and the NES cargo is disassembled in the cytoplasm as GTP hydrolysis on Ran is stimulated by RanGAP1 together with cytoplasmic RanBP1 or RanBP2 located at the cytoplasmic face of the nuclear pore complex (Fornerod et al., 1997a; Fornerod et al., 1997b; Fukuda et al., 1997; Askjaer et al., 1999; Kehlenbach et al., 1999; Roth et al., 2003; Bernad et al., 2004). Conversely, nuclear import complexes formed in the cytoplasm between proteins carrying a lysine-rich nuclear localization signal (NLS) and importins are dissociated in the nucleus by RanGTP, which binds to importin β (Görlich et al., 1996). Thus, nuclear RanGTP directs the selective nucleocytoplasmic transport of large proteins and associated macromolecules including RNA species (Clarke and Zhang, 2008).

During mitosis, when the compartmentalization of the nucleus is broken down in animal cells, RCC1 continues to associate with chromatin (Ohtsubo et al., 1989; Bischoff and Ponstingl, 1991; Carazo-Salas et al., 1999; Moore et al., 2002; Hutchins et al., 2004; Li and Zheng, 2004; Chen et al., 2007; Hitakomate et al., 2010) and generates a concentration gradient of RanGTP around the mitotic chromosomes that provides a directional signal for mitotic spindle assembly (Kalab et al., 2002; Caudron et al., 2005; Clarke, 2005b; Kaláb et al., 2006). Remarkably, beads coated with RCC1 to localize the generation of RanGTP are sufficient to induce spindle-like structures around them in M-phase *Xenopus* egg extract in the absence of chromatin (Halpin et al., 2011). Flattening the RanGTP gradient in this system makes bipolar spindle assembly around chromosomes dependent on the chromosome passenger complex (CPC), which is localized

This is an Open Access article distributed under the terms of the Creative Commons Attribution License (http://creativecommons.org/licenses/by/3.0), which permits unrestricted use, distribution and reproduction in any medium provided that the original work is properly attributed.

Journal of Cell Science

Journal of Cell Science

to centromeric chromatin (Maresca et al., 2009). Together, these experiments indicate that RanGTP provides a general spindle-promoting signal from chromatin while localized proteins stabilize specific interactions between chromosomes and spindle microtubules.

Importin α/β controls mitotic spindle assembly through binding to the nuclear localization signal (NLS) of spindle assembly factors (SAFs), including TPX2 (Gruss et al., 2001), NuMA (Nachury et al., 2001) and MCRS1 (Meunier and Vernos, 2011), and inhibits their functions. The inhibitory effects of importins α/β can be lifted by RanGTP through its specific binding to importin β and the release of SAFs (Gruss et al., 2001; Nachury et al., 2001; Wiese et al., 2001; Askjaer et al., 2002; Bamba et al., 2002). This provides a mechanism to spatially control the activity of SAFs through their proximity to chromosomes (Clarke and Zhang, 2008).

The role of nuclear export factors during mitosis is less well understood. A fraction of Crm1 locates to centrosomes and regulates centrosome duplication, maturation and mitotic spindle assembly by recruiting pericentrin, γ-tubulin and B23 (Liu et al., 2009; Rousselet, 2009). Kinetochore-localized Crm1, regulated by RanGTP, is responsible for RanBP2 and RanGAP1 recruitment to the kinetochore, thereby promoting the stabilization of kinetochore fibers and subsequent chromosome segregation in anaphase (Joseph et al., 2002; Arnaoutov et al., 2005). It has also been found that Crm1 tethers chromosomal passenger complex (CPC) to the centromere by interacting with a leucine-rich nuclear export signal (NES) of survivin during mitosis (Knauer et al., 2006). Furthermore, in yeast, the spindle assembly checkpoint (SAC) protein Mad1p is recruited onto the kinetochore upon SAC activation by Xpo1p/Crm1 and RanGTP. Mad1p contains a functional nuclear export signal (NES) that bind to Xpo1p, forming a trimeric complex with RanGTP (Scott et al., 2009). Since Crm1 is highly conserved among species from yeast to humans, it may be evolutionarily common that Crm1 contributes to spindle assembly by recruiting NES-containing SAFs to the spindle or kinetochore. This would be consistent with a model in which RanGTP, as well as causing the release of inhibited SAFs from importins during mitosis, also directs through Crm1 the formation of localized protein complexes that play roles in mitotic spindle assembly (Clarke, 2005a; Clarke and Zhang, 2008).

The breakdown of the nuclear envelope and the intermixing of nucleoplasm and cytoplasm present potential problems for the function of the Ran GTPase system during mitosis. The exposure of nuclear transport factors to all proteins carrying interaction motifs might prevent selective functioning of factors with roles during mitosis. In the case of Crm1, the protein might be bound up by soluble NES-containing proteins, potentially inhibiting any specific role on mitotic chromosomes or the spindle. Furthermore, if an SAF contains both NLS and NES motifs it could be bound by both importins and Crm1 in competition during mitosis.

In this report, we show that Crm1 is phosphorylated at serine 391 during mitosis by CDK1–cyclin-B (i.e. the CDK1 and cyclin B complex) and that this modification directs its spindle localization, which is required for proper spindle assembly, microtubule stability and chromosome alignment. Phosphorylation of Crm1 promotes its association with RanGTP and RanGAP1–RanBP2 on the spindle. These findings reveal that a mechanism by which a nuclear transport factor is controlled selectively during mitosis.

Results

Crm1 localizes to spindle microtubules and kinetochores in mitosis

Crm1 is present in the nucleus and on the nuclear envelope during interphase in human HeLa cells. We confirmed that, in mitosis, Crm1 localises to foci on condensed chromosomes identified as kinetochores by a Crest antibody (Arnaoutov et al., 2005; Liu et al., 2009). We also found that Crm1 is concentrated on the microtubules of the mitotic spindle (Fig. 1A,B). The kinetochore localization of Crm1 was apparent in cells arrested in mitosis by treatment with the microtubule poisons nocodazole or taxol, as well as monastrol, an inhibitor of the mitotic kinesin Eg5 (supplementary material Fig. S1). To confirm these localizations, we expressed a fusion protein of Crm1 coupled through its

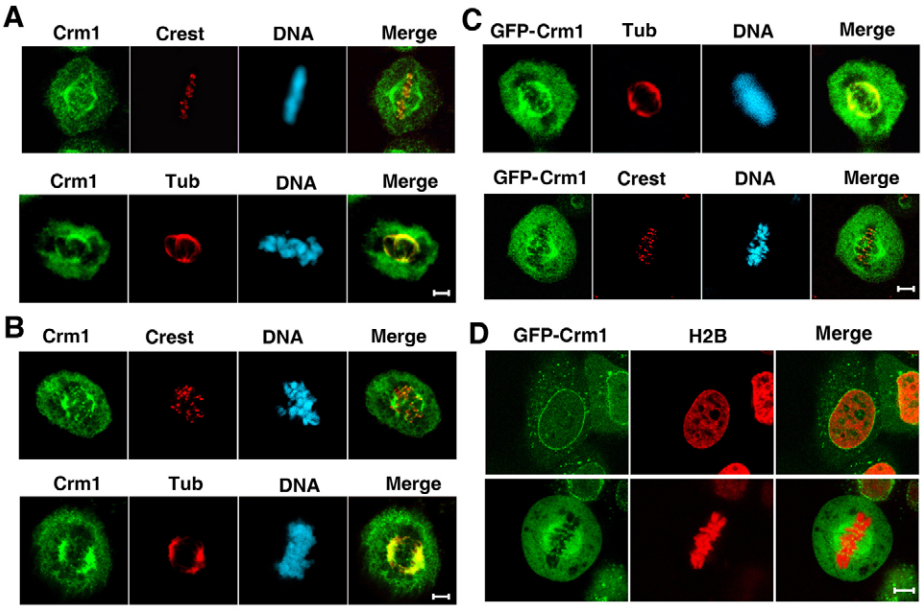

Fig. 1. A fraction of Crm1 localizes to the mitotic spindle as well as the kinetochore and centrosome. (**A**) Asynchronous HeLa cells were fixed with 3.7% PFA and stained for immunofluorescence using anti-N-terminal Crm1 (green) and anti-CREST or anti-tubulin antibodies (red). DNA was simultaneously counter-stained using DAPI. (**B**) Asynchronous HeLa cells were fixed with 3.7% PFA and stained for immunofluorescence using anti-C-terminal Crm1 (green) and anti-CREST or anti-tubulin (red) antibodies. DNA was simultaneously counter-stained using DAPI. (**C**) HeLa cells were transfected with GFP–Crm1. The cells were fixed 24 hours after transfection, and stained with anti anti-CREST or anti-tubulin antibody (red). DNA was visualized with DAPI. (**D**) HeLa cells were transfected with GFP–Crm1 (green) and RFP–H2B (red). The living cells were observed under the microscope 24 hours after transfection. Scale bars: 3 μm.

Journal of Cell Science

N-terminus to green fluorescent protein (GFP) in HeLa cells. Similar to localization of the endogenous protein detected by immunofluorescence, GFP–Crm1 was localized to mitotic spindles and kinetochores in fixed cells (Fig. 1C). Furthermore, we observed a very similar localization GFP–Crm1 to the mitotic spindle and kinetochores during mitosis as well as the nuclear envelope during interphase in living cells (Fig. 1D).

Crm1 is phosphorylated at serine 391 in mitosis

The distinct subcellular localization of Crm1 during mitosis suggested that it is regulated by post-translational modification. We found that most but not all Crm1 molecules were phosphorylated in mitotic cells and analysed by Western blotting following separation of proteins on Phos-tag gels that specifically retard phosphoproteins (Fig. 2A). A single retarded form was observed in cells arrested in mitosis with nocodazole for a prolonged period (17 h) or for a shorter period (2 h) after pre-synchronization at G1/S with thymidine (supplementary material Fig. S2A). Taxol (paclitaxel), a clinically important microtubule poison that also arrests cells in mitosis, similarly caused phosphorylation of Crm1 (supplementary material Fig. S2A). A single retarded form of Crm1 was observed in mitotic cells, consistent with a single major site of phosphorylation. By contrast, Crm1 phosphorylation was not detected in either non-mitotic adherent cells treated with nocodazole or in asynchronous cells treated with DNA damaging drugs (doxorubicin or hydroxyurea) or UV radiation (Fig. 2A).

To identify the potential site of phosphorylation, we examined the primary structure of Crm1 for possible phosphorylation sites. One site, serine 391, which has been identified in proteomic analyses of mitotic phosphoproteins (Daub et al., 2008; Dephoure et al., 2008; Olsen et al., 2010; Wang et al., 2010), is followed by

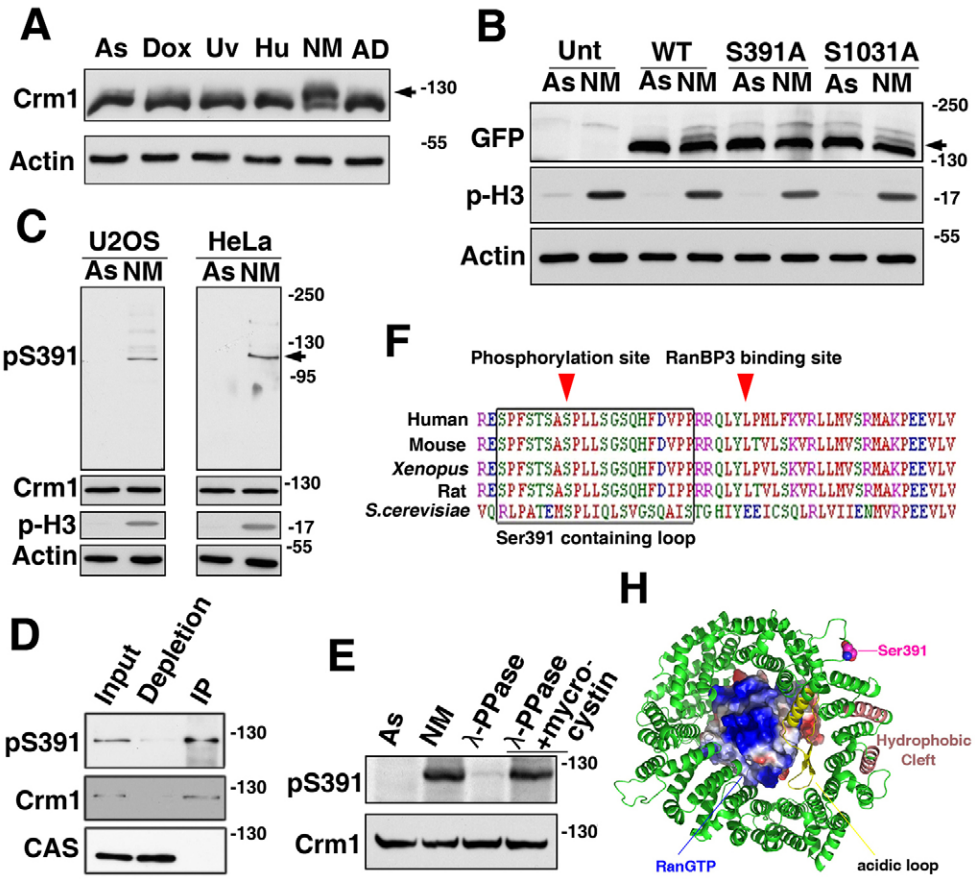

Fig. 2. Crm1 is phosphorylated at S391 in mitosis. (**A**) Asynchronous HeLa cells (As) were subjected to UV irradiation, or treated with doxorubicin (Dox) or hydroxyurea (Hu) to induce DNA damage. Cells arrested in mitosis by treatment with 100 ng/ml nocodazole for 17 h (NM) and the adherent cells (AD) were collected separately. Phosphorylation of Crm1 after the indicated treatment was visualized by the up-shift of the protein (arrow), detected by western blotting with anti-Crm1 antibody following separation on a Phos-tag acrylamide gel. Actin is shown as a control. (**B**) HeLa cells were transiently transfected with GFP–Crm1 WT, GFP–Crm1 S391A or GFP–Crm1 S1031A. After treatment with 100 ng/ml nocodazole for 17 h, samples were analyzed by Phos-tag acrylamide gel and immunoblotting with anti-GFP antibody. (**C**) Specificity of antibodies generated against the Crm1 phosphorylation site. HeLa and U2OS cells were grown in asynchronous culture (As) or treated with nocodazole for 17 h followed by shake-off (NM). Samples were analyzed by SDS–PAGE and immunoblotting with antibodies raised against the phosphorylated S391 site. (**D**) Nocodazole-arrested mitotic HeLa cell extracts were depleted with total Crm1 antibody and an equal proportion of supernatant and precipitates were examined by western blot, using CAS as a control. (**E**) Nocodazole-arrested mitotic HeLa cell extracts were treated with Lambda phosphatase (λ-PPase) or with both λ-PPase and mycrocystin, the λ-PPase inhibitor at 30℃ for 30 min. Asynchronous (AS) and nocodazole-arrested mitotic cell lysates (NM) were included as controls. (**F**) Alignment of Crm1 protein sequences in various mammals and *S. cerevisiae*. The phosphorylated residue and the nearby RanBP3-binding site are indicated by red arrows. (**H**) Diagram of Crm1 structure. CRM1 is shown as a ribbon/cartoon. The model is generated based on the crystal structure of the HIV-1 Rev-NES–CRM1–RanGTP nuclear export complex (PBD id: 3NBZ) using PyMOL software.

Journal of Cell Science

a proline, suggesting that it might be targeted by a proline-directed kinase like CDK1–cyclin-B. We mutated this site and another potential mitotic phosphorylation site, serine 1031, to non-phosphorylatable alanine residues and expressed the GFP-fused proteins in HeLa cells. Analysis of GFP–Crm1 proteins on Phos-tag gels followed by immunoblotting with an anti-GFP antibody showed that there was a retarded form of the protein in cells arrested in mitosis by nocodazole but not in asynchronous (interphase) cells that was abolished by the mutation for serine 391 (but not serine 1031) to alanine (Fig. 2B). Similar results were also obtained with Crm1 expressed with a hemagglutinin (HA) tag at the N-terminal of the protein (supplementary material Fig. S2B). These results indicate that Crm1 is phosphorylated at a single major site, serine 391, during mitosis in human cells.

To further study the regulation and function of Crm1 phosphorylation in mitosis, we synthesized a peptide containing phosphoserine 391 and used it to generate a specific polyclonal antibody. By western blotting, we confirmed that the antibody recognized a single major polypeptide in mitotically arrested HeLa and U2OS cells but not in asynchronous cells (Fig. 2C,D). This reactive band was removed by immunodepletion of Crm1 from mitotic cell extracts, confirming its identity as Crm1. We also treated the mitotic cell lysates with lambda PPase and found that the reactive band was abolished, whereas the reactive band was retained when the mitotic cell lysates were treated with both the PPase and its inhibitor mycrocystin, (Fig. 2E). Thus, we conclude that the antibody was specific to the phosphorylated Crm1 at S391.

Serine 391 is highly conserved among Crm1 homologues from yeast to humans (Fig. 2F). The site is located on a loop between the helix B of HEAT repeat 8 and helix A of HEAT repeat 9. Adjacent to this loop in the primary structure of Crm1, there is a binding region for RanBP3, which facilitates the binding of Crm1 with cargoes (Lindsay et al., 2001). Serine 391 is also close in the structure of Crm1 to the NES cargo-binding region (hydrophobic cleft) identified in the crystal structure of the RanGTP–Crm1 complex (Dong et al., 2009a; Dong et al., 2009b; Monecke et al., 2009) (Fig. 2H). Thus, we propose that phosphorylation of serine 391 might change the conformation of the S391-containing loop and thereby affect the cargo-binding region of Crm1 in complex with RanGTP.

CDK1–cyclin-B phosphorylates Crm1 at serine 391

To identify the kinase that phosphorylates Crm1 at S391, we treated nocodazole-arrested mitotic HeLa cells with a range of kinase inhibitors for a brief period (15 min). The phosphorylation status of Crm1 was analysed using the S391 phospho-specific antibody. We found that that the mitotic phosphorylation of Crm1 was inhibited by the CDK inhibitors Ro-3306 or purvalanol A (Fig. 3A), but not by Aurora B inhibitor ZM447439, consistent with a requirement for CDK1–cyclin-B (the major CDK in mitotically arrested cells) for Crm1 phosphorylation. Purvanalol A and particularly Ro-3306 induced exit of the cells from mitotic arrest even within 15 min judged by the mitotic phosphorylation of histone H3 at S10 and the loss of cyclin B, so this requirement might simply indicate a requirement for the mitotic state

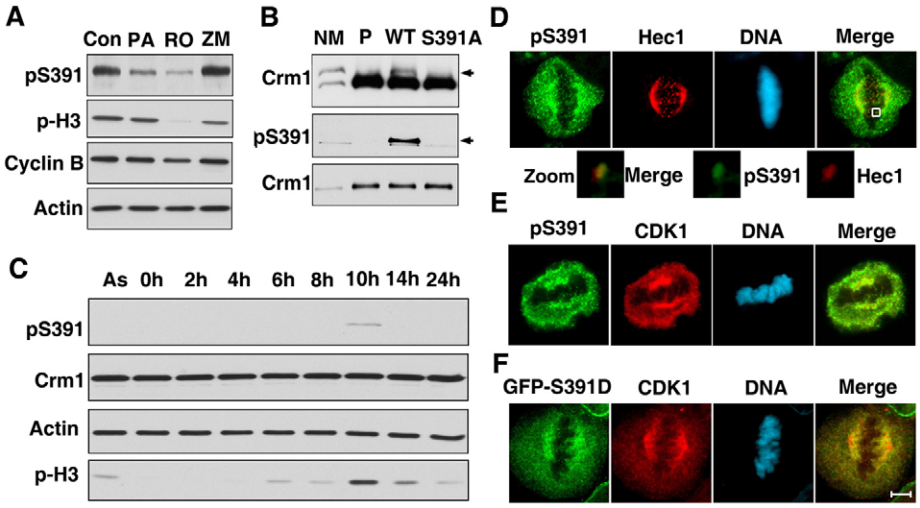

Fig. 3. CDK1 phosphorylates Crm1 and co-localizes on the mitotic spindle. (**A**) The CDK inhibitors Ro-3306 and purvalanol A significantly reduced the phosphorylation of Crm1 S391. HeLa cells were arrested by nocodazole for 17 h, which was followed by 9 μM Ro-3306, 10 μM purvalanol A and 2 μM ZM447439 treatment for 15 min. Mitotic cells were collected and analyzed by SDS–PAGE and immunoblotting using the phospho-specific antibody. (**B**) Crm1WT–His6 and Crm1 S391A–His6 were incubated for 1 h with recombinant CDK1–cyclin-B protein in the presence of an energy-regenerating system at 30℃. Samples were analyzed on a Phos-tag acrylamide gel or by normal SDS-PAGE and immunoblotting with anti-Crm1 or phospho-specific antibody. (**C**) Crm1 phosphorylation level is regulated through the cell cycle. HeLa cells were synchronized at the G1/S boundary by double thymidine block, then released into the cell cycle. Samples were analyzed by SDS–PAGE and immunoblotting using the phospho-specific antibody at the times shown after release from the block. (**D**) Intracellular localization of phospho-Crm1. Asynchronous HeLa cells were fixed with 3.7% PFA and stained for immunofluorescence using the phospho-specific antibody (green) and anti-Hec1 antibodies (red). DNA was simultaneously stained using DAPI. A small region, as indicated by the white box, was enlarged to show the overlap between pS391 and Hec1. (**E**) Relative localization of phospho-Crm1 and CDK1 at the mitotic spindle. Asynchronous HeLa cells were fixed with 3.7% PFA and stained for immunofluorescence using the phospho-specific antibody (green) and anti-CDK1 antibodies (red). DNA was simultaneously stained using DAPI. (**F**) Localizations of GFP–Crm1 S391D and CDK1 at the mitotic spindle. Asynchronous HeLa cells transfected with GFP–Crm1 S391D were fixed with 3.7% PFA and stained for immunofluorescence using anti-CDK1 antibodies (red). DNA was simultaneously stained using DAPI. Scale bar: 3 μm.

dependent on CDK1 activity (Fig. 3A). However, His_6-tagged recombinant Crm1, but not the non-phosphorylatable S391A mutant, was phosphorylated directly by purified CDK1–cyclin-B (Fig. 3B). These results indicate that CDK1–cyclin-B1 is responsible for the phosphorylation of Crm1 at S391 during mitosis.

To further characterize the cell-cycle-dependent phosphorylation of Crm1 at S391, HeLa cells were synchronized at the G1/S boundary using a double thymidine block, then released into the cell cycle. Cells synchronized in this way reached mitosis 10 hours after release from the thymidine block, as determined by the phosphorylation of histone H3 at S10 (Fig. 3C). In these cells, we found that Crm1 was phosphorylated at S391 coincident with H3 S10 in mitosis, while the total protein level of Crm1 was stable during the cell cycle (Fig. 3C).

Immunofluorescence microscopy using the S391 phospho-specific antibody indicated that phosphorylated Crm1 localized to both mitotic spindles and kinetochores, very similar to localization shown by Crm1 antibodies and GFP–Crm1. Co-detection with an antibody that detects the Ndc80 complex protein Hec1 on both spindle microtubules and kinetochores showed that Crm1 was localized close to Hec1 at kinetochores (Fig. 3D). Endogenous Crm1 phosphorylated at serine 391 and a GFP–Crm1 mutant with the serine 391 changed to aspartate, a phosphorylation-mimicking residue, also co-localized with CDK1 on the mitotic spindle (Fig. 3E,F).

To test the role of S391 phosphorylation in the localization of Crm1 in mitosis, we compared the localization in HeLa cells of GFP–Crm1, the non-phosphorylatable mutant S391A, and the phosphorylation-mimetic mutants S391D and S391E. We found that all were localized at both the mitotic spindle and the kinetochore but with some differences. The localization of GFP–Crm1 S391A on spindles was reduced compared to GFP–Crm1 WT and phosphorylation-mimetic mutants. Conversely, although the localization of the phosphorylation-mimetics GFP–Crm1 S391D and S391E to spindle microtubules was enhanced compared with GFP–Crm1 S391A, their localization to kinetochores was more variable, with some kinetochores showing stronger accumulation than others in the same cell (Fig. 4). One possible explanation might be that the attachment of microtubules to an individual kinetochore might affect phospho-Crm1 localization. However, we did not see a consistent difference between Crm1 localization to kinetochores in cells arrested in mitosis with nocodazole (no kinetochore attachment) compared to taxol (some kinetochore attachment) to support this conclusion (supplementary material Fig. S1B).

Phosphorylated Crm1 regulates spindle assembly and chromosome alignment

Crm1 has been reported to play a role in mitotic spindle assembly (Arnaoutov et al., 2005) and, as we observed that much of the Crm1 in mitotic cells is phosphorylated, we wondered whether the phosphorylation of Crm1 is important for the mitotic spindle assembly. To investigate this question, HeLa cells were transiently transfected with GFP–Crm1 WT, S391A, S391D and S391E plasmids for 24 h. We found that the morphology of the spindles in cells expressing phosphorylation-mimetic mutants GFP–Crm1 S391D and GFP–Crm1 S391E were more ‘robust’ than those in GFP–Crm1 S391A-expressing cells, with larger spindles and more intense microtubule staining (Fig. 4; Fig. 5A).

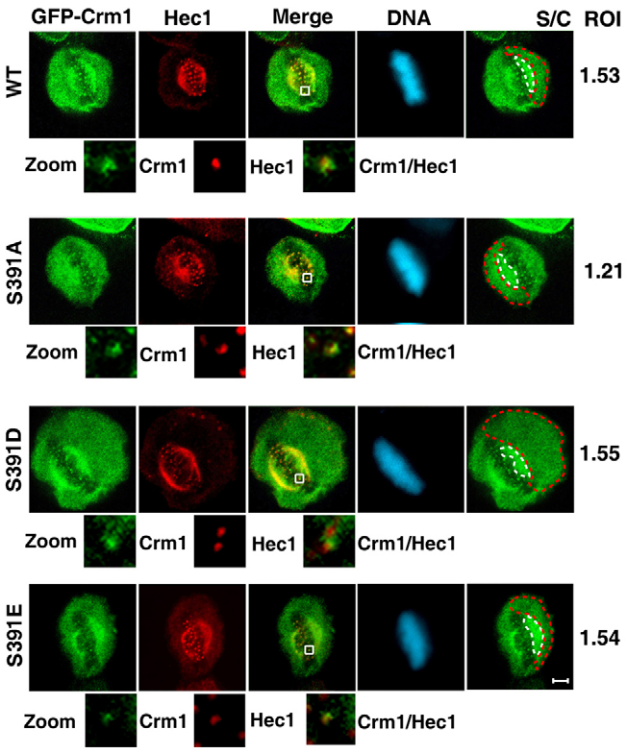

Fig. 4. Phosphorylation of Crm1 regulates its spindle localization but not kinetochore. Localizations of GFP–Crm1 (green) and Hec1 (red) at the mitotic spindle and kinetochore. Immunofluorescence of HeLa cells transiently transfected with GFP–Crm1 WT, GFP–Crm1 S391A, GFP–Crm1 S391D, GFP–Crm1 S391E, fixed with 3.7% PFA 24 h after transient transfection, followed by co-staining with anti-Hec1 antibodies (red). DNA was simultaneously stained using DAPI. The S/C ROI value, which represents the ratio of mean pixel density of the spindle ROI (indicated by white broken line) and cytoplasmic ROI (indicated by red broken line), was calculated to reflect the spindle localization level of GFP–Crm1 WT and its mutants. Scale bar: 3 μm.

By comparing the ratio of the mean pixel densities of the spindle and the cytoplasmic regions of interest (ROIs), we also found that the amount of the spindle-localized GFP–Crm1 S391A was significantly less than that of GFP–Crm1 WT, S391D or S391E (supplementary material Fig. S3). By measuring the pole-to-pole distance of the spindles, we found that the spindle length in cells expressing GFP–Crm1 WT, S391D or S391E were consistently longer than that in GFP–Crm1 S391A-expressing cells (Fig. 5B). By measuring the fluorescence intensity of the microtubule staining, we observed that the total number of spindle microtubules in GFP–Crm1 S391D and S391E-expressing cells was increased around 30% compared to wild-type cells. Conversely, the quality of the spindle microtubules in GFP–Crm1 S391A cells were significantly reduced, such that microtubule intensity was around 55% of that of the GFP–Crm1 WT cells and less than 50% of that in cells expressing the acidic mutants (Fig. 5C). In these experiments, the cells contained endogenous Crm1 (expected to be mostly phosphorylated), which might mitigate the effects of the transfected mutants. We therefore depleted endogenous Crm1 from HeLa cells by exposure to siRNA for 48 h prior to transient transfection of siRNA-resistant GFP–Crm1 WT, S391A, S391D, S391E plasmids for further 24 h. In siRNA-depleted cells, we found that the mitotic spindle was

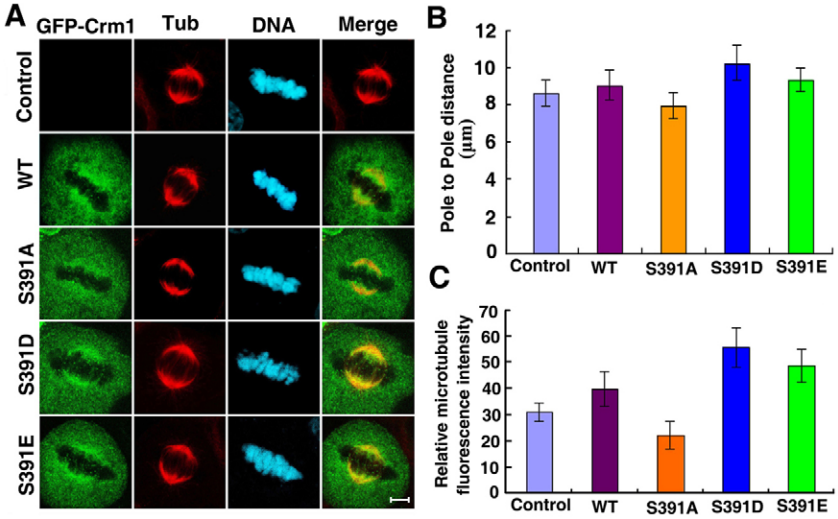

Fig. 5. Phospho-Crm1 regulates spindle assembly and controls spindle size. (**A**) Immunofluorescence of HeLa cells transiently transfected with GFP–Crm1 WT, GFP–Crm1 S391A, GFP–Crm1 S391D, GFP–Crm1 S391E plasmids. The HeLa cells were fixed 24 h after transfection. Overlay shows GFP–Crm1 (green) and tubulin (red). DNA was simultaneously stained using DAPI. The morphology of the spindles in cells overexpressing the phosphorylation-mimetic mutants GFP–Crm1 S391D and GFP–Crm1 S391E were much better than those in the S391A cells. Scale bar: 3 μm. (**B**) Pole-to-pole distance is decreased in cells transfected with GFP–Crm1 S391A compared with that in GFP–Crm1 S391D, GFP–Crm1 S391E and GFP–Crm1 WT. The pole-to-pole distance was measured by ZEN 2009. All the experiments were repeated at least three times, and more than 100 cells were measured for each sample. The data are mean ± s.d., ANOVA test results were $F=45.220$, $P=1.57\text{E-}26<0.05$. Thus, the length data among different groups were significantly different. Tukey's post-hoc test shows that $P_{(391A,Con)}=0.0118963315813639<0.05$, $P_{(391A,WT)}=2.12\text{E-}06<0.05$, $P_{(391A,391D)}=4.82\text{E-}13<0.05$, $P_{(391A,391E)}=4.79\text{E-}11<0.05$. (**C**) Microtubule intensity is decreased in cells transfected with GFP–Crm1 S391A compared with GFP–Crm1 S391D, GFP–Crm1 S391E and GFP–Crm1 WT. The relative microtubule intensity of a half-spindle was measured using Image J software. All the experiments were repeated at least three times. The data are mean ± s.d.

shortened in those cells expressing GFP–Crm1 S391A (supplementary material Fig. S4), similar to cells containing the endogenous Crm1 (Fig. 5C). This suggests that the presence of the endogenous Crm1 does not affect the results of the transfection of mutants. The S391A mutant is therefore likely to have a dominant inhibitory effect on spindle architecture when expressed at these levels.

Leptomycin B (LMB), a Crm1-specific inhibitor (Nishi et al., 1994), causes chromosome segregation defects, showing a role for Crm1 in this process (Arnaoutov et al., 2005). In order to check whether the phosphorylation of Crm1 affects chromosome alignment and segregation, we overexpressed exogenous GFP-tagged Crm1 and its mutants in HeLa cells. We observed that chromosome congression was disrupted in cells expressing GFP–Crm1 S391A and the numbers of cells with lagging chromosomes were significantly increased to around 30% of the total, six times more than those cells without expression of exogenous Crm1. Although the numbers of the cells with the chromosome misalignment were also increased to 13% in GFP–Crm1 WT, 11% in GFP–Crm1 S391D and 9% in GFP–Crm1 S391E overexpressing cells, there was a clear difference with the GFP–Crm1 S391A cells (Fig. 6). Through immuno-staining of Aurora-B to show the location of the centromeres, we measured the width of the chromosome plates of the cells overexpressing the Crm1 mutants. The results showed that the width of the Aurora B metaphase plate was significantly increased in GFP–Crm1 S391A cells (supplementary material Fig. S5). Taken together, these results indicate that phosphorylated Crm1 promotes chromosome alignment and the formation of the metaphase plate.

We also examined the stability of kinetochore microtubule bundles, or k-fibres, by cold-treating cells overexpressing the GFP-fused Crm1 proteins. It is known that kinetochore microtubules are relatively more stable to cooling on ice than non-kinetochore microtubules (Salmon and Begg, 1980; Rieder, 1981; DeLuca et al., 2002; Lampson and Kapoor, 2005). We, therefore, cooled cells for 10 min and performed immunofluorescence microscopy with an alpha tubulin antibody. We found that kinetochore microtubule bundles were abundant in the cells overexpressing GFP–Crm1 wild-type and phosphorylation-mimetic mutants, more than in cells without expression of GFP–Crm1. By contrast, the cells overexpressing nonphosphorylatable mutant GFP–Crm1 S391A had less kinetochore microtubule bundles (Fig. 7A). To test whether the increased spindle microtubule nucleation was due to the recruitment of SAFs by Crm1 through its NES-binding activity, we treated cells with leptomycin B (LMB) to block the interaction of Crm1 and NES cargoes. The result showed that kinetochore microtubule bundles were clearly reduced in LMB-treated cells compared to untreated cells (Fig. 7A). Taken together, these results confirm that phosphorylated Crm1 regulates the stability of k-fibres through a NES-type interaction with effector proteins.

To test whether the phosphorylated Crm1 directly regulates bipolar spindle assembly, we investigated bipolar spindle reformation in cells after depolymerization by cold treatment in nocodazole-arrested mitotic HeLa cells. We first treated the transfected cells with nocodazole to arrest cells in mitosis followed by incubation in medium on ice for 1 h to depolymerize the microtubules completely (supplementary material Fig. S6). The cells were then moved to medium pre-warmed at 37℃ and

Journal of Cell Science

Journal of Cell Science

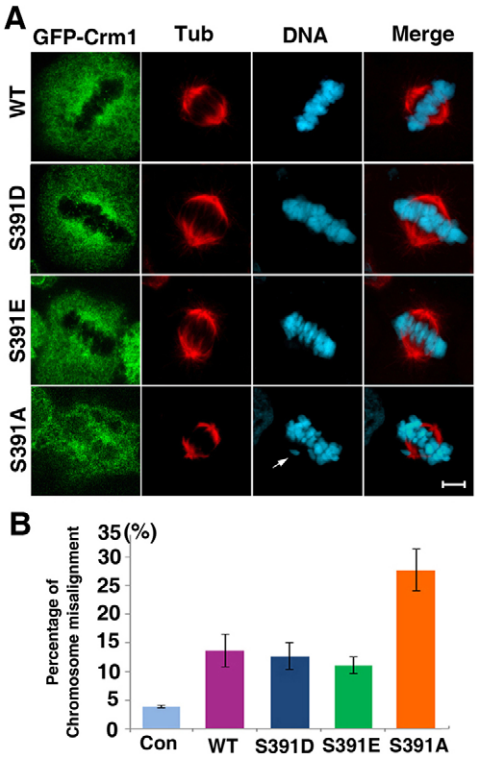

Fig. 6. Phospho-Crm1 is required for proper chromosome alignment. (**A**) Immunofluorescence of HeLa cells transiently transfected with GFP–Crm1 WT, GFP–Crm1 S391A, GFP–Crm1 S391D or GFP–Crm1 S391E plasmids. The HeLa cells were fixed 24 h after transfection. The overlay image shows GFP–Crm1 (green) and tubulin (red). DNA was simultaneously stained using DAPI. The white arrow indicates the misaligned chromosomes. Scale bar: 3 µm. (**B**) Chromosome misalignment is increased in cells transfected with GFP–Crm1 S391A. The percentage of chromosome misalignment for the cells described in A. All the experiments were repeated three times, and more than 300 cells were counted for each sample. The data are mean ± s.d.

incubated for a period to allow microtubule regrowth from kinetochores as well as centrosomes. The results showed that microtubules were nucleated quickly from both from kinetochore and centrosome, and the kinetochores were captured efficiently by microtubules in the cells expressing phosphorylation-mimetic GFP–Crm1 S391D, GFP–Crm1 S391E and GFP–Crm1 WT. Around 60% of these cells contain bipolar spindles. By contrast, microtubule nucleation and bipolar spindle formation was significantly inhibited in GFP–Crm1 S391A cells, some of the kinetochores were not properly captured by the microtubules. Only around 23% of the cells expressing GFP–Crm1 S391A contained bipolar spindles (Fig. 7B,C; supplementary material Fig. S7). These results indicate that phosphorylated Crm1 both promotes microtubule nucleation and facilitates the connection between the kinetochore and microtubules to promote bipolar spindle formation.

Phosphorylated Crm1 has higher affinity for RanGTP and promotes interaction with RanGAP1–RanBP2 in competition with importin β

In a co-precipitation assay, we found that phospho-Crm1 strongly bound RanGTP (RanQ69L) in mitosis (Fig. 8A). To test if the phosphorylation of Crm1 affects its interaction with RanGTP, lysates of mitotic HeLa cells transiently expressing GFP–Crm1 WT, S391A or S391D were precipitated using GFP-Trap beads in the presence of RanQ69L, a form stabilized in the GTP-bound conformation, followed by western blots using anti-Ran and GFP antibodies. We found that RanQ69L was abundant in the precipitate of GFP–Crm1 S391D, but less so in the precipitate of GFP–Crm1 S391A (Fig. 8B), suggesting that phosphorylation of Crm1 at S391 in mitosis enhances the binding of Crm1 to RanGTP. Consistent with this, non-phosphorylated GFP–Crm1 WT and GFP–Crm1 S391A had similar binding affinity to RanQ69L in interphase cells (supplementary material Fig. S8A).

The kinetochore and spindle localization of RanGAP1 (Joseph et al., 2002) requires Crm1 (Arnaoutov et al., 2005), suggesting a potential mechanism for the effect of Crm1 phosphorylation on spindle assembly. We found that Crm1 did indeed co-precipitate with RanGAP1 in a RanGTP-dependent manner in mitotic cell lysates (Fig. 8C), and this binding of Crm1 to RanGAP1 was disrupted by LMB (Fig. 8D). When the lysates were pretreated with λ-protein phosphatase (λ-PPase), it was found that the level of endogenous Crm1 precipitated by a RanGAP1 antibody in the presence of RanQ69L was strongly reduced (supplementary material Fig. S8B), indicating that the binding of Crm1 to RanGAP1 in mitosis is phosphorylation-dependent. The CDK1 inhibitor purvalanol A also inhibited the interaction of RanGAP1 with Crm1 in the lysate (supplementary material Fig. S8C). Moreover, in an immunoprecipitation assay in the presence of RanQ69L using GFP-Trap beads and lysates of mitotic HeLa cells stably expressing GFP–Crm1 WT, S391A or S391D, we found that RanQ69L, RanGAP1 and RanBP2 were more abundant in the precipitate of GFP–Crm1 WT and S391D, but less so in the precipitate of GFP–Crm1 S391A (Fig. 8E). Taken together, these results indicate that phosphorylation of Crm1 at S391 by CDK1–cyclin-B promotes the formation of a complex between RanGTP, Crm1, RanGAP1 and RanBP2.

Importin β regulates diverse aspects of mitosis including spindle formation, chromosome alignment, mitotic progression and RanGAP1 localization at kinetochores (Roscioli et al., 2012). We found that, in the absence of RanQ69L, RanGAP1 was complexed with importin β but not phospho-Crm1 in mitotic cell lysates; it is likely that endogenous RanGTP levels become lowered in these lysates during their preparation due to GTP hydrolysis on Ran. In the presence of added RanQ69L, however, RanGAP1 formed a complex with phospho-Crm1 but not importin β (Fig. 8F). These results indicate that, in the presence of RanGTP generated by RCC1 on mitotic chromosomes, RanGAP1 preferentially associates with phosphorylated Crm1 rather than importin β during mitosis.

To test whether the formation of the RanGTP–Crm1–RanGAP1–RanBP2 complex affects the recruitment of RanGAP1 and RanBP2 to the spindle, we overexpressed GFP-tagged phosphorylation-mimetic and non-phosphorylatable mutants to interfere the function of endogenous Crm1 in HeLa cells and co-stained for RanGAP1 or RanBP2 (Fig. 8G). The results showed that a significant fraction of both Crm1 and RanGAP1–RanBP2 were colocalized on the spindle. We observed that the amount of the non-phosphorylatable mutant Crm1 S391A on the spindle was reduced compared to the WT or phosphorylation-mimetic mutants, as noted previously, and the amount of localized RanGAP1 and RanBP2 correlated with GFP–Crm1, being reduced in cells expressing the GFP–Crm1

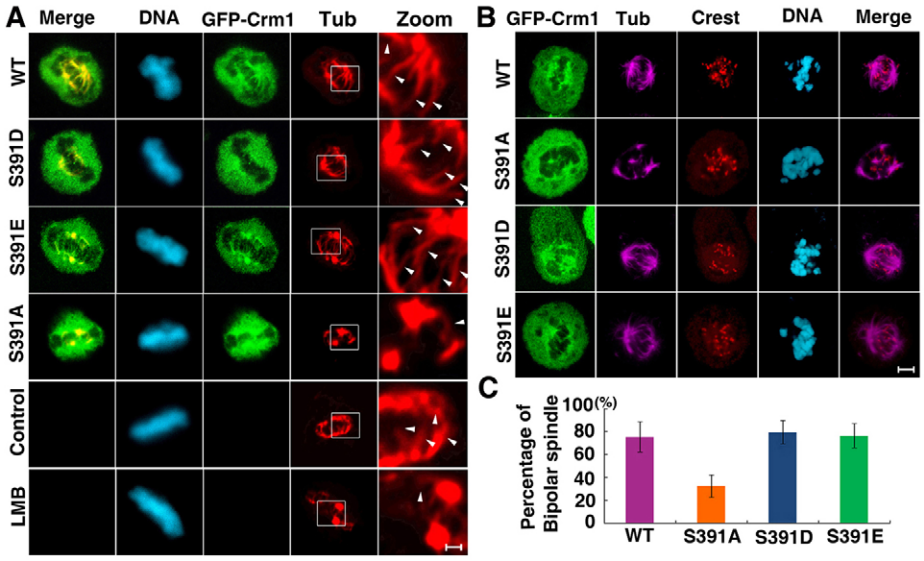

Fig. 7. Phospho-Crm1 is required for stable kinetochore microtubule formation and proper attachment between kinetochore and microtubule. (**A**) HeLa cells were treated with 10 nM leptomycin B (LMB) or transiently transfected with GFP–Crm1 WT, GFP–Crm1 S391A, GFP–Crm1 S391D, GFP–Crm1 S391E plasmids. The cells were incubated on ice for 10 min after 1 h treatment of LMB or 24 h after transfection. Cells were fixed with microtubule-stabilization buffer containing 0.2% Triton X-100 and 3.7% paraformaldehyde, followed by staining with anti-tubulin antibody (red). DNA was simultaneously stained using DAPI. A small region of the tubulin staining is shown at higher magnification to see the cold-resistant microtubules more clearly (arrowheads). Scale bar: 3 μm. (**B**) HeLa cells were transiently transfected with GFP–Crm1 WT, GFP–Crm1 S391A, GFP–Crm1 S391D or GFP–Crm1 S391E plasmids. The cells were arrested by nocodazole 24 h after transfection, followed by incubation in medium on ice for 1 h to depolymerize the microtubules. Then the cells were moved to pre-warmed medium at 37℃ and incubated for 12 min to allow microtubule regrow from the kinetochores as well as the centrosome. The cells were finally double-stained with anti-tubulin (purple) and anti-CREST (red) antibodies, after fixation. Scale bar: 3 μm. (**C**) Percentage of bipolar spindle formation for the cells described in B. The bipolar spindle assembly is inhibited in cells transfected with GFP–Crm1 S391A. All the experiments were repeated three times, and more than 300 cells were counted in each sample. The data are mean ± s.d.

S391A mutant. In these cells, both the mutant Crm1 protein and RanGAP1–RanBP2 were more evenly distributed in the cytoplasm with only a small amount concentrated on the microtubules of the spindle, as measured in a cross section of the spindle (Fig. 8G). These results indicate that the phosphorylation of Crm1 enhances the recruitment of RanGAP and RanBP2 to the mitotic spindle and thereby promotes spindle assembly.

Discussion

Ran GTPase and its binding proteins regulate mitotic spindle assembly. A RanGTP gradient model has been proposed in which the chromosome-localized nucleotide exchange factor RCC1 generates a high concentration of RanGTP around the condensed chromosomes. The concentration of RanGTP decreases with distance from the chromosomes, forming an intracellular gradient of diffusible RanGTP that provides an intracellular directional signal that directs spindle assembly. High concentrations of RanGTP are thought to induce microtubule nucleation in the vicinity of chromosomes by releasing spindle assembly factors from inhibitory complexes with importins (Clarke and Zhang, 2008).

An alternative or refined model for the role of RanGTP in mitotic spindle assembly involves formation and localization of multiprotein complexes by RanGTP (Zhang et al., 1999; Joseph et al., 2002; Arnaoutov et al., 2005; Tedeschi et al., 2007; Torosantucci et al., 2008; Rousselet, 2009). In this protein localization model, RanGTP directs the recruitment of spindle assembly factors (SAFs) to some specific structures, such as centrosome and kinetochore. Ran itself localizes in part to the mitotic apparatus, particularly the polar/kinetochore microtubules and the spindle poles (Zhang et al., 1999; Trieselmann and Wilde, 2002). In addition, several Ran system proteins including importin β, Crm1, RanBP1, RanGAP1, RanBP2, CAS/CSE1 and Rae1 have been reported to locate to the mitotic apparatus (Joseph et al., 2002; Arnaoutov et al., 2005; Blower et al., 2005; Tedeschi et al., 2007). In the case of importin β, its association with the spindle may allow it to deliver SAFs to their correct location until they are released locally by RanGTP (Tahara et al., 2008). A similar role has been proposed for importin β in targeting proteins to chromatin during nuclear envelope formation at telophase (Zhang et al., 2002; Lu et al., 2012).

In this report, we show that, in addition to the localization of Crm1 to the kinetochore (Joseph et al., 2002; Arnaoutov et al., 2005) and centrosome (Liu et al., 2009; Rousselet, 2009) previously reported, a fraction of Crm1 localizes to mitotic spindle microtubules and, with the cooperation of RanGTP, recruits RanGAP1 and RanBP2. Although RanGAP1 and RanBP2 are thought to play an important role in mitotic spindle assembly, their biochemical function is not yet certain. RanBP2 may enhance the stimulation of GTP hydrolysis on Ran by RanGAP1, reduce local RanGTP concentrations, and thereby promote the release of active SAFs from Crm1. Alternatively, RanBP2–RanGAP1 may act as an effector of RanGTP, for instance through the E3 Sumo-ligase activity or cyclophilin-like domain of RanBP2 (Arnaoutov et al., 2005; Clarke, 2005a). Sumoylation of Topo II alpha by RanBP2 in mitosis is required for its proper localization to inner centromeres and to ensure the

Journal of Cell Science

chromosomal stability to suppress tumorigenesis (Dawlaty et al., 2008). Similarly, sumoylation activity by RanBP2–RanGAP1 could modify other factors involved in microtubule dynamics, for instance, to promote microtubule nucleation and stabilization.

Although the Ran system is crucial for diverse cellular functions including nuclear transport, DNA replication, nuclear assembly and mitotic spindle assembly, how the system is controlled during mitosis has been unclear. One example that has been discovered is the regulation of RCC1, which is

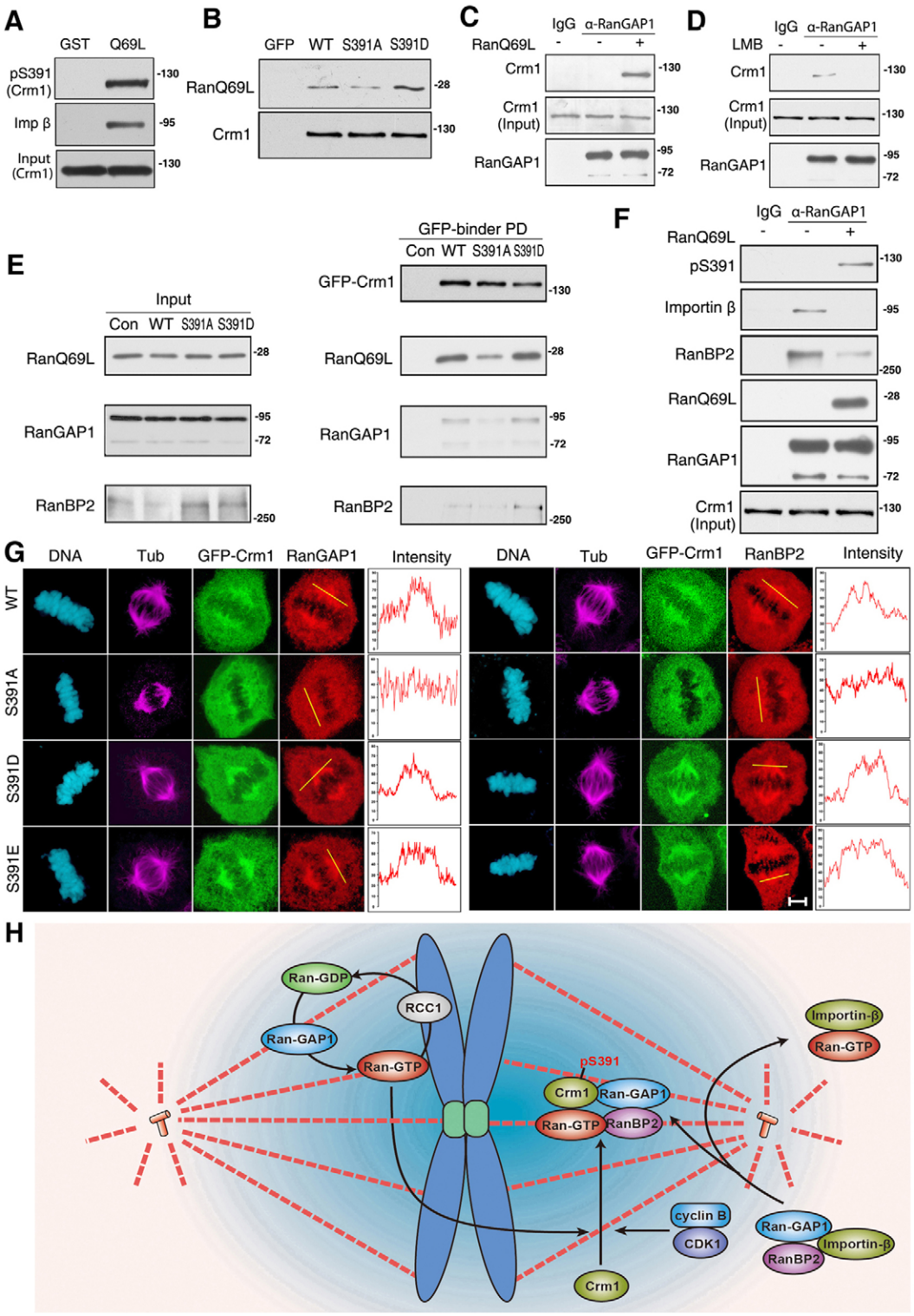

Fig. 8. See next page for legend.

Journal of Cell Science

Journal of Cell Science

phosphorylated by CDK1–cyclin-B1 in its N-terminal tail. This region of RCC1 contains the NLS, and phosphorylation disrupts the binding of importin α/β, thereby promoting the dynamic interaction of RCC1 with mitotic chromosomes (Hutchins et al., 2004; Li and Zheng, 2004). Phosphorylation of RCC1 might be important to ensure that it continues to interact chromosomes efficiently during prometaphase when RanGTP is dispersed after nuclear envelope breakdown. Phosphorylation therefore can provide a cargo-specific mechanism to alter the interaction with a transport factor during mitosis to prevent it from being bound up inappropriately.

We now show that phosphorylation of the transport factor Crm1 by CDK1–cyclin-B at a single major site, S391, alters the molecular interactions made by Crm1 in mitosis. Phosphorylation of Crm1 enhances its interaction with RanGTP and promotes the recruitment of RanGAP1–RanBP2 to the mitotic spindle. It seems that RanGAP1 preferentially associates with phosphorylated Crm1 rather than importin β, so CDK1–cyclin-B in conjunction with RanGTP can promote the mitotic function of Crm1 by overcoming the opposing effects of importin β (Roscioli et al., 2012) on RanGAP1–RanBP2 localization and function. This illustrates how phosphorylation can direct the molecular interactions made by a transport factor in order for it accomplish a specific role during mitosis. Indeed, it will be of interest to elucidate at the structural level how the phosphorylation of Crm1 affects its cargo-binding properties in order to select specific mitotic partners.

In summary, we have shown the subcellular localization and function of Crm1 in mitosis are regulated by CDK1–cyclin-B (Fig. 8H). When a cell enters mitosis, Crm1 is phosphorylated by CDK1–cyclin-B. This phosphorylation enhances the formation of a complex with RanGTP and RanGAP1–RanBP2. Simultaneously, RanGTP generated by RCC1 on chromosomes lifts the inhibition of SAFs, including RanGAP1–RanBP2, by importin β. Thus, phosphorylated Crm1 recruits RanGAP1–RanBP2 to the mitotic spindle and kinetochores in a RanGTP-dependent manner.

Fig. 8. Phosphorylation of Crm1 enhances formation of the RanGTP–Crm1–RanGAP1–RanBP2 complex. (**A**) Phospho-Crm1 interacts with RanGTP during mitosis. HeLa cells were arrested in mitosis by treatment with 100 ng/ml nocodazole for 17 h. GST and GST–RanQ69L were incubated with mitotic cell lysates for 1 h and then precipitated with glutathione–Sepharose beads. The precipitates were immunoblotted for S391-phosphorylated Crm1 with importin β as a positive control. (**B**) Phospho-Crm1 has a higher affinity for RanGTP. HeLa cells transfected with GFP–Crm1 WT, GFP–Crm1 S391A or GFP–Crm1 S391D were arrested in mitosis by treatment with 100 ng/ml nocodazole for 17 h. GFP–Crm1 was precipitated from the mitotic (NM) cells using GFP trap beads in the presence of 2 μM RanQ69L; the precipitates were immunoblotted for Ran and GFP, respectively. (**C**) The interaction of Crm1 with RanGAP1 during mitosis is dependent on RanGTP. HeLa cells were arrested in mitosis by treatment with 100 ng/ml nocodazole for 17 h. RanGAP1 was precipitated from the mitotic (NM) cells using anti-RanGAP1 antibody in the presence or absence of 2.5 μM RanQ69L, and precipitates were immunoblotted for Crm1 and RanGAP1. IgG was used as a control for the precipitation. Cell lysates (Input) used for the precipitations are shown in the middle panel. (**D**) Leptomycin B (LMB) disrupts the interaction of Crm1 and RanGAP1 in mitosis. HeLa cells were arrested in mitosis by treatment with 100 ng/ml nocodazole for 17 h and were then treated with 10 nM LMB for 3 h. RanGAP1 was precipitated from the mitotic (NM) cells with 2.5 μM RanQ69L using anti-RanGAP1 antibody in the presence or absence of 10 nM LMB. IgG was used as a control for the precipitation. Cell lysates (Input) used for the precipitations are shown in the middle panel. (**E**) Phospho-Crm1 has a higher affinity for RanGTP and RanGAP1. HeLa cells stably expressing GFP–Crm1 WT, GFP–Crm1 S391A and GFP–Crm1 S391D were arrested in mitosis by treatment with 100 ng/ml nocodazole for 17 h. GFP–Crm1 was precipitated from mitotic (NM) cells using GFP beads in the presence of 2 μM RanGTP and immunoblotted for GFP, RanGAP1, Ran and RanBP2. Cell lysates (Input) used for the precipitations are shown in the left panels. (**F**) RanGTP releases RanGAP1 from importin β and promotes formation of the RanGAP1–pS391-Crm1 complex. HeLa cells were arrested in mitosis by treatment with 100 ng/ml nocodazole for 17 h. RanGAP1 was precipitated from mitotic (NM) cells using anti-RanGAP1 antibody in the presence or absence of 2.5 μM RanQ69L and immunoblotted for pS391-Crm1 and importin β, RanBP2, RanQ69L and RanGAP1. IgG was used as a control for the precipitation. Cell lysates (Input) used for the precipitations are shown in the bottom panel. Scale bar: 3 μm. (**G**) HeLa cells were transfected with GFP–Crm1, GFP–Crm1 S391A, GFP–Crm1 S391D or GFP–Crm1 S391E plasmids. The cells were fixed 24 h after transfection, before staining with anti-RanGAP1 antibody (red). The relative intensity of RanGAP1 or RanBP2 localization on a cross section of the spindles, indicated by the straight line on the RanGAP1 and RanBP2 images, respectively, is plotted. Intensities were measured using Image J. (**H**) A model for the role of Crm1 and its phosphorylation by CDK1–cyclin-B in the regulation of the mitotic spindle assembly. RCC1 (a guanine-nucleotide-exchange factor) localizes on mitotic chromosomes and generates RanGTP. Both importin β, possibly together with importin α, and Crm1 are major mitotic effectors of RanGTP. Crm1 is phosphorylated at S391 by CDK1 and localizes to the mitotic spindle. Meanwhile, RanGAP1 and RanBP2 are both mitotic spindle assembly factors (SAFs) and form a complex in mitosis; however, this complex is bound by importins and inhibited in the cytoplasm in absence of RanGTP. Once the complex of RanGAP1–RanBP2 bound with importins randomly moves to the mitotic spindle region, the interaction of RanGTP with importin β causes the release of RanGAP1–RanBP2. In the presence of RanGTP, phospho-Crm1 forms a complex with RanGAP1–RanBP2 and recruits RanGAP1–RanBP2 to the mitotic spindle to regulate the spindle assembly.

Materials and Methods

Antibodies and reagents

The following antibodies were used for immunoblotting and immunofluorescence: Crm1 (mouse monoclonal, raised against N-terminal of Crm1) (BD Pharmingen); Hec1 (9G3, ab3631, Abcam); mab414 (Convance); RanBP2 (Rabbit polyclonal, a kind gift from Richard Wong, Kanazawa University); RanBP2 (Monoclonal, a kind gift from Richard Wong, Kanazawa University); Crm1 (rabbit polyclonal, raised against C-terminal of Crm1), RanGAP1, cyclin B1, CDK1, GFP (Santa Cruz Biotechnology); actin (Sigma); histone H3 phospho-S10 (Millipore); Rabbit polyclonal phospho-specific antibodies were generated against Crm1 phosphopeptides (pS391 Crm1, FSTSAS*PLLSGSQ, where S* represents the phosphorylated residue) (Moravian Biotechnology, Brno, Czech Republic). Phospho-specific antibodies were affinity purified by two rounds of negative selection against non-phosphorylated peptide followed by one round of positive selection with phosphorylated peptide.

Cell culture, synchronization and transfection

HeLa cells were cultured in DMEM, containing 10% fetal serum at 37℃. To generate stable clones of HeLa cells expressing GFP–Crm1 (wild-type, S391A and S391D), HeLa cells were transfected with indicated constructs. Single clones were selected in G418 (800 μg/ml, Calbiochem). To analyze the cell cycle regulated phosphorylation, cells were synchronized at the G1/S boundary by double thymidine block then released for the indicated times, which involved incubation with 2 mM thymidine for 16 h, followed by an 8 h release into normal medium before the addition of 2 mM thymidine for a further 16 h. To arrest cells in mitosis, cells were treated with the specified concentration of nocodazole or taxol for the times given. Transient cDNA transfections were carried out on cells using Lipofectamine 2000 (Invitrogen) according to the manufacturer's instructions.

Crm1 phosphorylation assay using Phos-tag SDS–PAGE

Phos-tag is a phosphate-binding reagent at neutral pH (physiological pH) through its Mn^{2+}-dependent interaction with phosphomonoester dianions bound to Ser, Thr and Tyr residues (Kinoshita et al., 2006). Protein samples were analyzed on 8% SDS–PAGE with 25 mM Phos-tag acrylamide (Phos-tag, Hiroshima, Japan) added to the resolving gel. During electrophoresis, the phosphorylated proteins were specifically retarded by the Phos-tag. The gels were soaked in transfer buffer with 1 mM EDTA for 10 min, followed by 10 min incubation in transfer buffer without EDTA before wet transfer.

Immunoprecipitation

For RanGAP1 precipitations, cells were lysed in IP buffer (40 mM HEPES pH 7.5, 120 mM NaCl, 0.2% CHAPS, 1 mM EDTA, 50 mM NaF, 10 mM

β-glycerophosphate, 0.2 mM PMSF, 1 mg/ml each pepstatin, leupeptin and aprotinin and 1 mM DTT). A total of 1 mg of lysate was incubated with 20 µg RanGAP1 goat antibody (Santa Cruz Biotechnology) in the presence or absence of 2 µM RanQ69L at 4℃ for 2 h and then with 20 µl prewashed protein-G–Sepharose, 4℃, 1 h. Precipitates were washed three times for 5 min before addition of SDS sample buffer. For GFP-tagged precipitations, cells were lysed in IP buffer. A total of 1.5 mg lysates was incubated with 15 µl GFP-trap agarose (ChromoTek) in the presence of 2 µM RanQ69L at 4℃ for 2 h. Precipitates were washed three times for 5 min each in IP buffer.

In vivo and *in vitro* kinase assays

For kinase inhibitor assay in cells, the kinase inhibitors were added to nocodazole arrested mitotic cells for 15 min. The mitotic cells were washed off and lysed in 2×SDS-lysis buffer (100 mM Tris pH6.8, 4% SDS and 20% glycerol). Samples were analyzed by SDS–PAGE and immunoblotting. Kinase inhibitors were used at the following concentrations: 10 µM purvalanol A, 2 µM ZM447439, 9 µM Ro-3306. Crm1–His_6 was expressed in *E. coli* BL21 and purified by nickel–agarose affinity chromatography. For western analysis of Crm1 phosphorylation *in vitro*, 500 ng Crm1–His_6 was incubated with 50 ng human recombinant CDK1–cyclin-B (Upstate) for 60 min at 30℃ in kinase buffer (50 mM Tris–HCl pH 7.5, 10 mM $MgCl_2$ and 10 mM DTT) plus 100 µM ATP.

Immunofluorescence and microscopy quantifications

Cells on coverslips were washed with PBS, followed by either immediately fixed with 3.7% paraformaldehyde, or incubated in PEM buffer (100 mM PIPES pH 6.9, 2 mM EGTA, 1 mM $MgSO_4$) containing 0.2% Triton X-100 for 1 min at room temperature and then fixed with 3.7% paraformaldehyde. After fixation, cells were washed three times in TBS-T, and blocked with 5% BSA for 30 min, incubated with primary antibodies overnight at 4℃, washed with TBS, incubated with secondary antibodies for 1 h, washed with TBS. For the assessment of microtubule regrowth, 1 µM nocodazole was added 24 h after transfection, and incubation was continued for 6 h at 37℃. The cells were washed twice with cold complete DMEM medium to remove the nocodazole, with further incubation in DMEM medium for 1 h on ice. The medium was replaced by pre-warmed complete DMEM media, and cells were incubated at 37℃ for the indicated time. The cells were processed for immunofluorescence. For the assessment of microtubule cold stability, the cells were incubated for 10 min on ice 24 h after transfection or 6 h after incubation with 10 nM leptomycin B (LMB). Images were acquired using a Zeiss LSM 510 Meta system and Zeiss LSM 710 Duo scan system. Images from different channels were captured simultaneously and automatically. To show DNA staining more clearly, the DNA in blue were manually pseudo-colored to cyan. The fluorescence intensity was measured by Image J software (NCBI). Spindle size was measured by ZEN 2009.

Acknowledgements

We thank all the other members in our laboratories for their comments, Lindsey Allan in Dundee for her initial work identifying Crm1 phosphorylation, Richard Wong (Kanazawa University) for kind gift of RanBP2 antibodies and Fangjin Chen (College of Chemistry and Molecular Engineering, Peking University) for preparing Fig. 2F.

Author contributions

Experiments were performed by Z.W. with assistance from Q.J. Z.W., P.R.C. and C.Z wrote the manuscript. The study was conceived and jointly supervised by P.R.C. and C.Z.

Funding

This work was supported by the State Key Basic Research and Development Plan [grant number 2010CB833705 to C.Z.]; the National Natural Science Foundation of China (NSFC) [grant numbers 31071188, 31030044 and 90913021 to C.Z.]; and a two-year visiting studentship from China Scholarship Council (CSC) to work in Dundee (to Z.W.). P.R.C. was supported by the Biotechnology and Biological Sciences Research Council (BBSRC).

Supplementary material available online at
http://jcs.biologists.org/lookup/suppl/doi:10.1242/jcs.126854/-/DC1

References

Arnaoutov, A., Azuma, Y., Ribbeck, K., Joseph, J., Boyarchuk, Y., Karpova, T., McNally, J. and Dasso, M. (2005). Crm1 is a mitotic effector of Ran-GTP in somatic cells. *Nat. Cell Biol.* **7**, 626-632.

Askjaer, P., Bachi, A., Wilm, M., Bischoff, F. R., Weeks, D. L., Ogniewski, V., Ohno, M., Niehrs, C., Kjems, J., Mattaj, I. W. et al. (1999). RanGTP-regulated interactions of CRM1 with nucleoporins and a shuttling DEAD-box helicase. *Mol. Cell. Biol.* **19**, 6276-6285.

Askjaer, P., Galy, V., Hannak, E. and Mattaj, I. W. (2002). Ran GTPase cycle and importins alpha and beta are essential for spindle formation and nuclear envelope assembly in living Caenorhabditis elegans embryos. *Mol. Biol. Cell* **13**, 4355-4370.

Bamba, C., Bobinnec, Y., Fukuda, M. and Nishida, E. (2002). The GTPase Ran regulates chromosome positioning and nuclear envelope assembly in vivo. *Curr. Biol.* **12**, 503-507.

Bernad, R., van der Velde, H., Fornerod, M. and Pickersgill, H. (2004). Nup358/RanBP2 attaches to the nuclear pore complex via association with Nup88 and Nup214/CAN and plays a supporting role in CRM1-mediated nuclear protein export. *Mol. Cell. Biol.* **24**, 2373-2384.

Bischoff, F. R. and Ponstingl, H. (1991). Catalysis of guanine nucleotide exchange on Ran by the mitotic regulator RCC1. *Nature* **354**, 80-82.

Bischoff, F. R., Klebe, C., Kretschmer, J., Wittinghofer, A. and Ponstingl, H. (1994). RanGAP1 induces GTPase activity of nuclear Ras-related Ran. *Proc. Natl. Acad. Sci. USA* **91**, 2587-2591.

Blower, M. D., Nachury, M., Heald, R. and Weis, K. (2005). A Rae1-containing ribonucleoprotein complex is required for mitotic spindle assembly. *Cell* **121**, 223-234.

Carazo-Salas, R. E., Guarguaglini, G., Gruss, O. J., Segref, A., Karsenti, E. and Mattaj, I. W. (1999). Generation of GTP-bound Ran by RCC1 is required for chromatin-induced mitotic spindle formation. *Nature* **400**, 178-181.

Caudron, M., Bunt, G., Bastiaens, P. and Karsenti, E. (2005). Spatial coordination of spindle assembly by chromosome-mediated signaling gradients. *Science* **309**, 1373-1376.

Chen, T., Muratore, T. L., Schaner-Tooley, C. E., Shabanowitz, J., Hunt, D. F. and Macara, I. G. (2007). N-terminal alpha-methylation of RCC1 is necessary for stable chromatin association and normal mitosis. *Nat. Cell Biol.* **9**, 596-603.

Clarke, P. R. (2005a). The Crm de la crème of mitosis. *Nat. Cell Biol.* **7**, 551-552.

Clarke, P. R. (2005b). Cell biology. A gradient signal orchestrates the mitotic spindle. *Science* **309**, 1334-1335.

Clarke, P. R. and Zhang, C. (2008). Spatial and temporal coordination of mitosis by Ran GTPase. *Nat. Rev. Mol. Cell Biol.* **9**, 464-477.

Daub, H., Olsen, J. V., Bairlein, M., Gnad, F., Oppermann, F. S., Körner, R., Greff, Z., Kéri, G., Stemmann, O. and Mann, M. (2008). Kinase-selective enrichment enables quantitative phosphoproteomics of the kinome across the cell cycle. *Mol. Cell* **31**, 438-448.

Dawlaty, M. M., Malureanu, L., Jeganathan, K. B., Kao, E., Sustmann, C., Tahk, S., Shuai, K., Grosschedl, R. and van Deursen, J. M. (2008). Resolution of sister centromeres requires RanBP2-mediated SUMOylation of topoisomerase IIalpha. *Cell* **133**, 103-115.

DeLuca, J. G., Moree, B., Hickey, J. M., Kilmartin, J. V. and Salmon, E. D. (2002). hNuf2 inhibition blocks stable kinetochore-microtubule attachment and induces mitotic cell death in HeLa cells. *J. Cell Biol.* **159**, 549-555.

Dephoure, N., Zhou, C., Villén, J., Beausoleil, S. A., Bakalarski, C. E., Elledge, S. J. and Gygi, S. P. (2008). A quantitative atlas of mitotic phosphorylation. *Proc. Natl. Acad. Sci. USA* **105**, 10762-10767.

Dong, X., Biswas, A. and Chook, Y. M. (2009a). Structural basis for assembly and disassembly of the CRM1 nuclear export complex. *Nat. Struct. Mol. Biol.* **16**, 558-560.

Dong, X., Biswas, A., Süel, K. E., Jackson, L. K., Martinez, R., Gu, H. and Chook, Y. M. (2009b). Structural basis for leucine-rich nuclear export signal recognition by CRM1. *Nature* **458**, 1136-1141.

Fornerod, M., Ohno, M., Yoshida, M. and Mattaj, I. W. (1997a). CRM1 is an export receptor for leucine-rich nuclear export signals. *Cell* **90**, 1051-1060.

Fornerod, M., van Deursen, J., van Baal, S., Reynolds, A., Davis, D., Murti, K. G., Fransen, J. and Grosveld, G. (1997b). The human homologue of yeast CRM1 is in a dynamic subcomplex with CAN/Nup214 and a novel nuclear pore component Nup88. *EMBO J.* **16**, 807-816.

Fukuda, M., Asano, S., Nakamura, T., Adachi, M., Yoshida, M., Yanagida, M. and Nishida, E. (1997). CRM1 is responsible for intracellular transport mediated by the nuclear export signal. *Nature* **390**, 308-311.

Görlich, D., Panté, N., Kutay, U., Aebi, U. and Bischoff, F. R. (1996). Identification of different roles for RanGDP and RanGTP in nuclear protein import. *EMBO J.* **15**, 5584-5594.

Gruss, O. J., Carazo-Salas, R. E., Schatz, C. A., Guarguaglini, G., Kast, J., Wilm, M., Le Bot, N., Vernos, I., Karsenti, E. and Mattaj, I. W. (2001). Ran induces spindle assembly by reversing the inhibitory effect of importin alpha on TPX2 activity. *Cell* **104**, 83-93.

Halpin, D., Kaláb, P., Wang, J., Weis, K. and Heald, R. (2011). Mitotic spindle assembly around RCC1-coated beads in Xenopus egg extracts. *PLoS Biol.* **9**, e1001225.

Hitakomate, E., Hood, F. E., Sanderson, H. S. and Clarke, P. R. (2010). The methylated N-terminal tail of RCC1 is required for stabilisation of its interaction with chromatin by Ran in live cells. *BMC Cell Biol.* **11**, 43.

Hutchins, J. R., Moore, W. J., Hood, F. E., Wilson, J. S., Andrews, P. D., Swedlow, J. R. and Clarke, P. R. (2004). Phosphorylation regulates the dynamic interaction of RCC1 with chromosomes during mitosis. *Curr. Biol.* **14**, 1099-1104.

Joseph, J., Tan, S. H., Karpova, T. S., McNally, J. G. and Dasso, M. (2002). SUMO-1 targets RanGAP1 to kinetochores and mitotic spindles. *J. Cell Biol.* **156**, 595-602.

Journal of Cell Science

Kalab, P., Weis, K. and Heald, R. (2002). Visualization of a Ran-GTP gradient in interphase and mitotic Xenopus egg extracts. *Science* **295**, 2452-2456.
Kaláb, P., Pralle, A., Isacoff, E. Y., Heald, R. and Weis, K. (2006). Analysis of a RanGTP-regulated gradient in mitotic somatic cells. *Nature* **440**, 697-701.
Kehlenbach, R. H., Dickmanns, A., Kehlenbach, A., Guan, T. and Gerace, L. (1999). A role for RanBP1 in the release of CRM1 from the nuclear pore complex in a terminal step of nuclear export. *J. Cell Biol.* **145**, 645-657.
Kinoshita, E., Kinoshita-Kikuta, E., Takiyama, K. and Koike, T. (2006). Phosphate-binding tag, a new tool to visualize phosphorylated proteins. *Mol. Cell. Proteomics* **5**, 749-757.
Knauer, S. K., Bier, C., Habtemichael, N. and Stauber, R. H. (2006). The Survivin-Crm1 interaction is essential for chromosomal passenger complex localization and function. *EMBO Rep.* **7**, 1259-1265.
Lampson, M. A. and Kapoor, T. M. (2005). The human mitotic checkpoint protein BubR1 regulates chromosome-spindle attachments. *Nat. Cell Biol.* **7**, 93-98.
Li, H. Y. and Zheng, Y. (2004). Phosphorylation of RCC1 in mitosis is essential for producing a high RanGTP concentration on chromosomes and for spindle assembly in mammalian cells. *Genes Dev.* **18**, 512-527.
Lindsay, M. E., Holaska, J. M., Welch, K., Paschal, B. M. and Macara, I. G. (2001). Ran-binding protein 3 is a cofactor for Crm1-mediated nuclear protein export. *J. Cell Biol.* **153**, 1391-1402.
Liu, Q., Jiang, Q. and Zhang, C. (2009). A fraction of Crm1 locates at centrosomes by its CRIME domain and regulates the centrosomal localization of pericentrin. *Biochem. Biophys. Res. Commun.* **384**, 383-388.
Lu, Q., Lu, Z., Liu, Q., Guo, L., Ren, H., Fu, J., Jiang, Q., Clarke, P. R. and Zhang, C. (2012). Chromatin-bound NLS proteins recruit membrane vesicles and nucleoporins for nuclear envelope assembly via importin-α/β. *Cell Res.* **22**, 1562-1575.
Maresca, T. J., Groen, A. C., Gatlin, J. C., Ohi, R., Mitchison, T. J. and Salmon, E. D. (2009). Spindle assembly in the absence of a RanGTP gradient requires localized CPC activity. *Curr. Biol.* **19**, 1210-1215.
Meunier, S. and Vernos, I. (2011). K-fibre minus ends are stabilized by a RanGTP-dependent mechanism essential for functional spindle assembly. *Nat. Cell Biol.* **13**, 1406-1414.
Monecke, T., Güttler, T., Neumann, P., Dickmanns, A., Görlich, D. and Ficner, R. (2009). Crystal structure of the nuclear export receptor CRM1 in complex with Snurportin1 and RanGTP. *Science* **324**, 1087-1091.
Moore, W., Zhang, C. and Clarke, P. R. (2002). Targeting of RCC1 to chromosomes is required for proper mitotic spindle assembly in human cells. *Curr. Biol.* **12**, 1442-1447.
Nachury, M. V., Maresca, T. J., Salmon, W. C., Waterman-Storer, C. M., Heald, R. and Weis, K. (2001). Importin beta is a mitotic target of the small GTPase Ran in spindle assembly. *Cell* **104**, 95-106.
Nishi, K., Yoshida, M., Fujiwara, D., Nishikawa, M., Horinouchi, S. and Beppu, T. (1994). Leptomycin B targets a regulatory cascade of crm1, a fission yeast nuclear protein, involved in control of higher order chromosome structure and gene expression. *J. Biol. Chem.* **269**, 6320-6324.
Ohtsubo, M., Okazaki, H. and Nishimoto, T. (1989). The RCC1 protein, a regulator for the onset of chromosome condensation locates in the nucleus and binds to DNA. *J. Cell Biol.* **109**, 1389-1397.
Olsen, J. V., Vermeulen, M., Santamaria, A., Kumar, C., Miller, M. L., Jensen, L. J., Gnad, F., Cox, J., Jensen, T. S., Nigg, E. A. et al. (2010). Quantitative phosphoproteomics reveals widespread full phosphorylation site occupancy during mitosis. *Sci. Signal.* **3**, ra3.
Ossareh-Nazari, B., Bachelerie, F. and Dargemont, C. (1997). Evidence for a role of CRM1 in signal-mediated nuclear protein export. *Science* **278**, 141-144.
Rieder, C. L. (1981). The structure of the cold-stable kinetochore fiber in metaphase PtK1 cells. *Chromosoma* **84**, 145-158.
Roscioli, E., Di Francesco, L., Bolognesi, A., Giubettini, M., Orlando, S., Harel, A., Schininà, M. E. and Lavia, P. (2012). Importin-β negatively regulates multiple aspects of mitosis including RANGAP1 recruitment to kinetochores. *J. Cell Biol.* **196**, 435-450.
Roth, P., Xylourgidis, N., Sabri, N., Uv, A., Fornerod, M. and Samakovlis, C. (2003). The Drosophila nucleoporin DNup88 localizes DNup214 and CRM1 on the nuclear envelope and attenuates NES-mediated nuclear export. *J. Cell Biol.* **163**, 701-706.
Rousselet, A. (2009). Inhibiting Crm1 causes the formation of excess acentriolar spindle poles containing NuMA and B23, but does not affect centrosome numbers. *Biol. Cell* **101**, 679-693.
Salmon, E. D. and Begg, D. A. (1980). Functional implications of cold-stable microtubules in kinetochore fibers of insect spermatocytes during anaphase. *J. Cell Biol.* **85**, 853-865.
Scott, R. J., Cairo, L. V., Van de Vosse, D. W. and Wozniak, R. W. (2009). The nuclear export factor Xpo1p targets Mad1p to kinetochores in yeast. *J. Cell Biol.* **184**, 21-29.
Stade, K., Ford, C. S., Guthrie, C. and Weis, K. (1997). Exportin 1 (Crm1p) is an essential nuclear export factor. *Cell* **90**, 1041-1050.
Tahara, K., Takagi, M., Ohsugi, M., Sone, T., Nishiumi, F., Maeshima, K., Horiuchi, Y., Tokai-Nishizumi, N., Imamoto, F., Yamamoto, T. et al. (2008). Importin-beta and the small guanosine triphosphatase Ran mediate chromosome loading of the human chromokinesin Kid. *J. Cell Biol.* **180**, 493-506.
Tedeschi, A., Ciciarello, M., Mangiacasale, R., Roscioli, E., Rensen, W. M. and Lavia, P. (2007). RANBP1 localizes a subset of mitotic regulatory factors on spindle microtubules and regulates chromosome segregation in human cells. *J. Cell Sci.* **120**, 3748-3761.
Torosantucci, L., De Luca, M., Guarguaglini, G., Lavia, P. and Degrassi, F. (2008). Localized RanGTP accumulation promotes microtubule nucleation at kinetochores in somatic mammalian cells. *Mol. Biol. Cell* **19**, 1873-1882.
Trieselmann, N. and Wilde, A. (2002). Ran localizes around the microtubule spindle in vivo during mitosis in Drosophila embryos. *Curr. Biol.* **12**, 1124-1129.
Wang, Y. T., Tsai, C. F., Hong, T. C., Tsou, C. C., Lin, P. Y., Pan, S. H., Hong, T. M., Yang, P. C., Sung, T. Y., Hsu, W. L. et al. (2010). An informatics-assisted label-free quantitation strategy that depicts phosphoproteomic profiles in lung cancer cell invasion. *J. Proteome Res.* **9**, 5582-5597.
Wiese, C., Wilde, A., Moore, M. S., Adam, S. A., Merdes, A. and Zheng, Y. (2001). Role of importin-beta in coupling Ran to downstream targets in microtubule assembly. *Science* **291**, 653-656.
Zhang, C., Hughes, M. and Clarke, P. R. (1999). Ran-GTP stabilises microtubule asters and inhibits nuclear assembly in Xenopus egg extracts. *J. Cell Sci.* **112**, 2453-2461.
Zhang, C., Hutchins, J. R., Mühlhäusser, P., Kutay, U. and Clarke, P. R. (2002). Role of importin-beta in the control of nuclear envelope assembly by Ran. *Curr. Biol.* **12**, 498-502.

Journal of Cell Science